Supporting Information

A Hg(I) corrugated sheet assembled by adjuvant dioxole groups and Hg···π interactions

Francisco Sánchez-Férez[a], Xavier Solans-Monfort,[a] Teresa Calvet[b], Mercè Font-Bardia[c], Josefina Pons[a,]*

[a]Departament de Química, Universitat Autònoma de Barcelona, 08193-Bellaterra, Barcelona, Spain

[b]Departament de Mineralogia, Petrologia i Geologia Aplicada, Universitat de Barcelona, Martí i Franquès s/n, 08028 Barcelona, Spain.

[c]Unitat de Difracció de Raig-X, Centres Científics i Tecnològics de la Universitat de Barcelona (CCiTUB), Universitat de Barcelona, Solé i Sabarís, 1-3, 08028 Barcelona, Spain

Experimental

Materials and general details

Hg(II) acetate ($Hg(OAc)_2$), 1,3-benzodioxole-5-carboxylic acid (Piperonylic acid, HPip) and 4,4'-bipyridine (4,4'-bipy) ligands, and N,N-dimethylformamide (DMF) as solvent were purchased from Sigma-Aldrich (Darmstadt, Germany). All of them were used without further purification. All reactions and manipulation were carried out in a Digitheat-TFT furnace (JP Selecta) using sealed vials at 105°C under autogenous pressure. Elemental analyses (EA; C, H, N) were carried on a Euro Vector 3100 instrument. The FTIR-ATR spectra were recorded on a Perkin Elmer spectrometer, equipped with a universal attenuated total reflectance (ATR) accessory with diamond window in the range 4000-500 cm^{-1}. ^1H NMR spectrum was recorded on an NMR Bruker Ascend 300 MHz spectrometer in DMSO-d_6 solution at RT. All chemical shifts (δ) are given in ppm.

Synthesis of $[Hg_2(\mu\text{-Pip})_2]$ (**2**)

65.3 mg of **1** (0.0950 mmol) were added to 5 mL of DMF at 105 °C in a 10 mL vial and was stirred for 10 min until its complete dissolution. Then, the mixture was sealed, kept under autogenous pressure at 105 °C for 2 h and cooled to room temperature. The resulting single crystals of **P1B** (45.5 mg) were removed from the mixture and the solution was stand for 19 days until suitable crystals of **2** were formed. Yield: 10.1 mg (42.3%) (respect to **1**). Elem. Anal. Calc. for $C_{16}H_{10}Hg_2O_8$ (731.42 $g{\cdot}mol^{-1}$): C 26.27; H 1.38. Found C 26.12; H 1.15. ATR-FTIR (wavenumber, cm^{-1}): 3104(w) - 3052(w) [υ_{ar}(C-H)], 2996(w) - 2919(w) [υ_{al}(C-H)], 1614(w), 1580(s) [υ_{as}(COO)], 1548(sh.) [υ(C=C/C=N)], 1499(m), 1478(m), 1431(s) [υ_s(COO)], 1404(m), 1374(w), 1359(w), 1324(m), 1296(s), 1243(s), 1201(m), 1167(m), 1122(m), 1106(m), 1073(m), 1031(s) [δ_{ip}(C-H)], 927(m), 913(s), 869(sh.), 832(m), 821(m), 804(m), 767(s) [δ_{oop}(C-H)], 721(m), 676(m), 631(w), 583(m), 540(m), 505(w). ^1H NMR (300 MHz; DMSO-d_6; 298 K): δ = 6.08 [4H, s, O-CH_2-O], 6.96 [2H, d, ^3J = 8.3 Hz, O_2C-C-CH-C*H*], 7.35 [2H, d, ^4J = 1.4 Hz, O_2C-C-C*H*-CO], 7.53 [2H, dd, ^3J = 8.1 Hz, ^4J = 1.6 Hz, O_2C-C-C*H*-CH].

FTIR-ATR

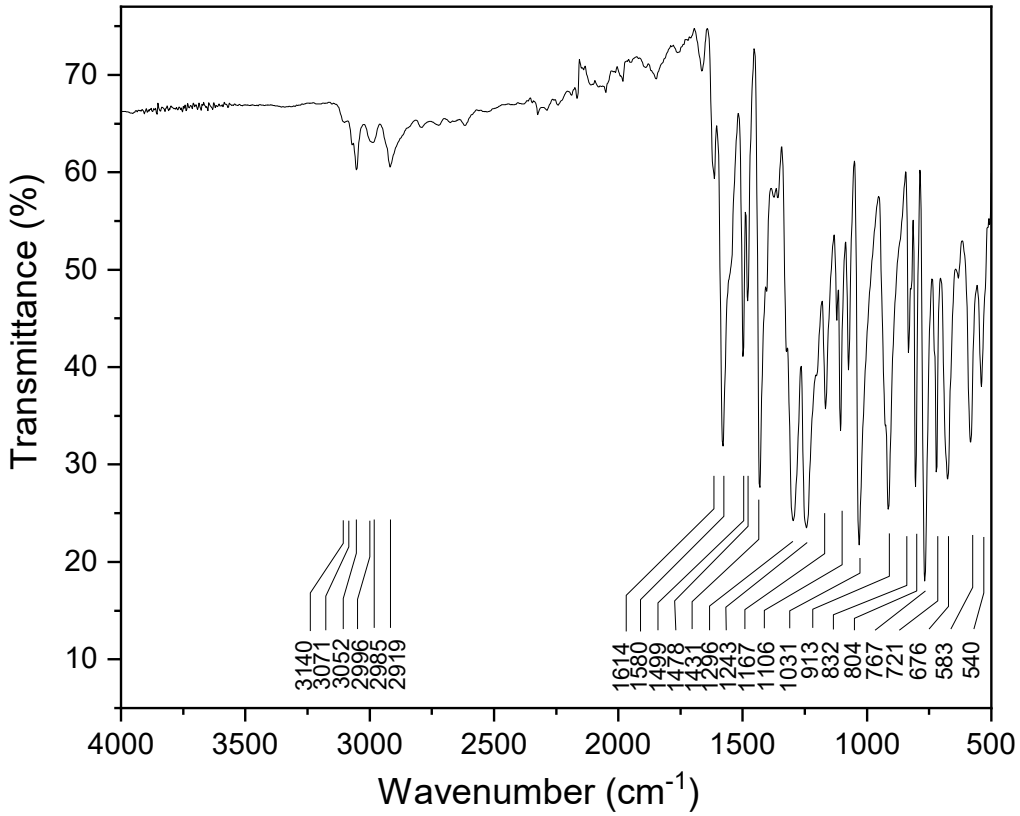

Figure S1. FTIR-ATR spectrum of $[Hg_2(\mu\text{-Pip})_2]$ (**2**).

^{1}H NMR spectroscopy

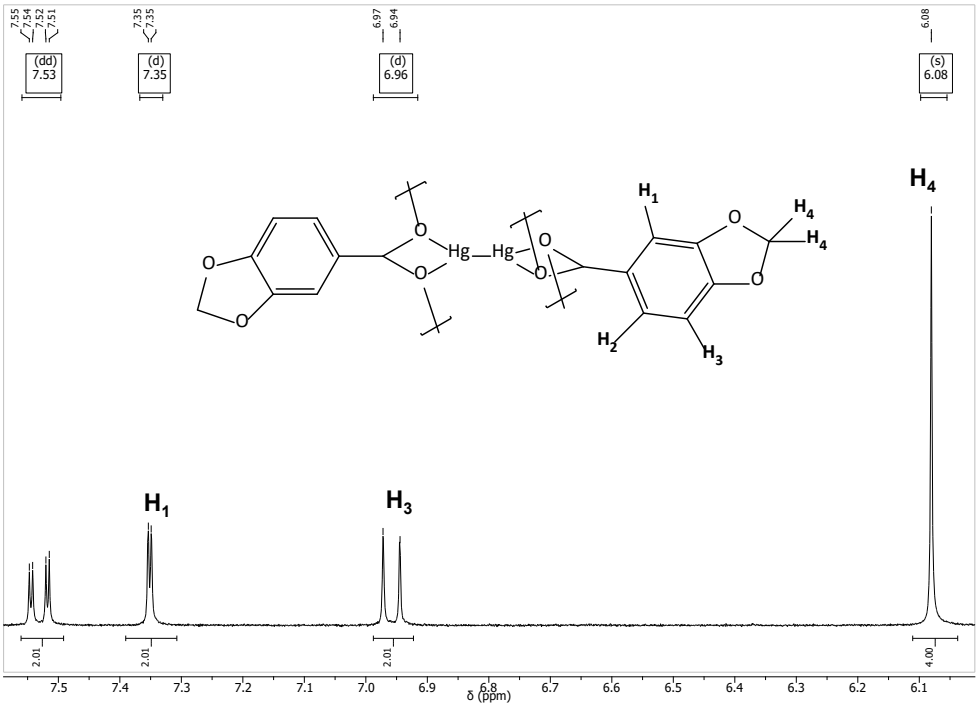

Figure S2. ^{1}H NMR spectrum of $[Hg_2(\mu\text{-Pip})_2]$ (**2**) in DMSO-d_6 at 298K.

X-Ray crystal Structure Data and Structural analysis of 2

A colorless prism-like specimen was used for the X-ray crystallographic analysis. The X-ray intensity data were measured on a D8 Venture system equipped with a multilayer monochromator and a Mo microfocus (λ = 0.71073 Å). The frames were integrated with the Bruker SAINT software package using a narrow-frame algorithm. The integration of the data using a monoclinic unit cell yielded 4,482 independent reflections (average redundancy 4.085, R_{sig} = 2.60%) and 4,279 (95.47%) were greater than 2σ($|F|^2$). The RMS deviation in the largest hole was 0.157 $e^-/Å^3$.

The structure of was solved and refined using the Bruker SHELXTL Software Package (version-2018/3).[1] The final cell constants and volume are based upon the refinement of the XYZ-centroids of reflections above 20 σ(I). Data were corrected for absorption effects using the multi-scan method (SADABS), Crystal data and relevant details of structure refinement is reported in Table S1. Complete information about the crystal structure and molecular geometry is available in CIF format as Supporting Information. CCDC number 2155639 (**2**). Molecular graphics were generated with Mercury 2021.3.0 software[2] or Moldraw 2.0 Version H1[3] using POV-Ray image package.[4] Color codes for all molecular graphics: Suva grey (Hg), red (O), grey (C) and white (H). Hirshfeld surface of the tetrameric unit [$Hg_4(Pip)_4$] with its 2D fingerprint plot have been generated using CrystalExplorer 21.5[5] to display the region involved in Hg···C contacts and identify its contribution in the contact surface area.

Hirshfeld surface analysis and 2D fingerprint plot

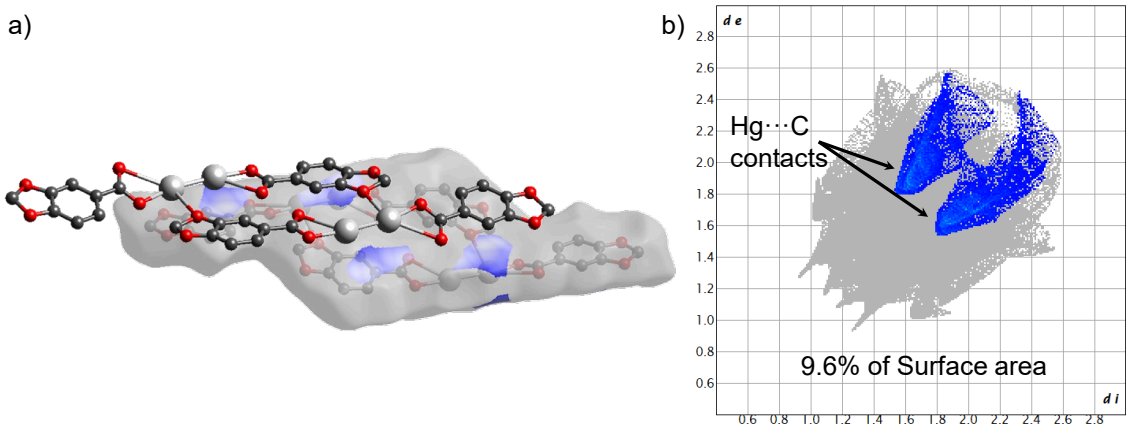

Figure S3. a) Hirshfeld surface representation and b) 2D fingerprint plot of **2** highlighting Hg···C contacts within the chains. Hydrogen atoms have been omitted for clarity.

Table S1. Crystal structure refinement parameters of **2**.

	2
Empirical formula	$C_{16}H_{10}Hg_2O_8$
Formula weigh	731.42
T (K)	100(2)
Wavelength (Å)	0.71073
System, space group	Monoclinic, $P2_1/n$
Unit cell dimensions	
a (Å)	12.9072(7)
b (Å)	6.2378(3)
c (Å)	19.2643(10)
α (°)	90
β (°)	98.396(2)
γ (°)	90
V (Å3)	1534.39(14)
Z	4
Dcalc (g cm^3)	3.166
μ (mm^{-1})	20.034
F (000)	1320
Crystal size (mm^3)	0.300x0.120x0.080
hkl ranges	-18≤h≤15 -8≤k≤8
θ range (°)	3.367 to 30.665
Reflections collected/ unique/[R_{int}]	18309/4482/0.0282
Completeness to θ (%)	96.6
Absorption Correction	Semi-empirical from equivalents
Max. and min. transmis.	0.7461 and 0.3123
Refinement method	Full matrix least-squares on $\|F\|^2$
Data/restrains/parameters	4482/0/229
Goodness of fit (GOF) on $\|F\|^2$	1.146
Final R indices [I>2σ(I)]	R_1 = 0.0181,
R indices (all data)	R1 = 0.0197
Extinction coefficient	n/a
Largest. Diff. peak and hole (e $Å^{-3}$)	1.629 and -1.538

Table S2. Bond lengths (Å), bond angles (°) and intermolecular interactions in **2**.

Bond lengths and Hg···O interactions				
Hg(1)-O(1)	2.132(2)	Hg(2)···O(6)[a]		2.891(2) [a]
Hg(1)···O(2)	2.742(2)[a]	Hg(1)-Hg(2)		2.51602(18)
Hg(1)···O(5)	3.013(2)[a]	Hg(1)···O(7)[a]		3.081(2) [a]
Hg(1)···O(6)	2.782(2)[a]	Hg(2)···O(4)[a]		3.132(2) [a]
Hg(2)-O(5)	2.126(2)			
Bond angles				
O(1)-Hg(1)-Hg(2)	175.56(6)	O(1)-Hg(1)-O(7)		87.66(7)
O(2)-Hg(1)-Hg(2)	123.79(5)	O(2)-Hg(1)-O(5)		74.70(6)
O(5)-Hg(1)-Hg(2)	169.26(6)	O(2)-Hg(1)-O(6)		134.70(6)
O(6)-Hg(1)-Hg(2)	98.54(5)	O(2)-Hg(1)-O(7)		122.44
O(5)-Hg(2)-Hg(1)	169.26(6)	O(5)-Hg(1)-O(6)		78.86(6)
O(6)-Hg(2)-Hg(1)	140.60(4)	O(5)-Hg(1)-O(7)		140.35(6)
O(7)-Hg(1)-Hg(2)	92.97(4)	O(6)-Hg(1)-O(7)		63.94(6)
O(4)-Hg(2)-Hg(1)	95.05(4)	O(4)-Hg(2)-O(5)		75.64(7)
O(1)-Hg(1)-O(2)	52.61(8)	O(4)-Hg(2)-O(6)		118.81(6)
O(1)-Hg(1)-O(5)	75.84(8)	O(5)-Hg(2)-O(6)		50.14(7)
O(1)-Hg(1)-O(6)	85.69(8)			
Intermolecular Interaction	H···A (Å)	D···A (Å)	D-H (Å)	>D-H···A (°)
C8-H8···O2	2.377	3.325(3)	0.950	176.44
Hg···π interactions				
Cg(I)···Hg(J)	Cg···Hg[b]	MeJ_Perp[c]		β[d]
Cg(1)···Hg(1)	3.720	3.342		26.04
Cg(2)···Hg2	3.446	3.318		15.67

[a]Hg(I)-O bonds that pertain to the secondary coordination. [b]Cg···Hg = distance (Å) between ring centroid and Hg(I) center. [c]MeJ_Perp = the perpendicular distance (Å) of Hg(I) on ring Cg(I). [d]Offset angle: β = angle Cg(I)-Cg(J) and normal to plane I (°). Cg(1) = C2-C3-C4-C5-C7-C8; Cg(2) = C(10)-C(11)-C(12)-C(14)-C(15)-C(16).

Computational Details

All calculations were performed with CRYSTAL17 package and using the X-Ray determined structure. With the aim of analyzing the importance of the considered structure, optimizations of the atomic positions at different levels of theory were carried out. The geometry optimization implied some structure reorganization and particularly a shortening of the Hg···π interaction and an elongation of the tetrameric units formation Hg···O_{COO} distance. However, the effect on the interaction energies and QTAIM analysis was minor and same conclusions could be drawn with any of the considered structures (X-ray or optimized). In any case, we decided that the analysis at the X-ray structure is more relevant and thus, all values reported in the main text correspond to the experimental structure. Both the topological analysis and the

interaction energy between nearby dimers is performed at the B3LYP-D2[6–8] level of theory. Main group elements are represented with Pople's 6-311G(d,p)[9] basis sets, while Hg is described with the Hay Wadt pseudopotential and the associated 64-4(31d) basis sets adapted for periodic calculations.[10] These basis sets are of the same quality to those used recently to describe the crystal structure of several [Hg(L)X_2] complexes and particularly, Hg is described with the same basis set in the two cases.[11] The interaction energies between dimers is determined as the energy difference between an isolated dimer and the model including two $Hg_2(Pip)_2$ units.[12] We also report the obtained values without D2 Grimme's empirical correction to analyze the importance of dispersion forces and particularly the Hg···π interaction that is essentially not taken into account at the B3LYP level of theory. A 4x4x4 Monkhorst−Pack K-point mesh was used in the periodic calculations to sample the Brillouin zone.

Table S3. Bader's Atoms In Molecules (QTAIM) analysis of the Hg···X interactions. ρ, $\nabla^2\rho$ and G are the electron density, the Laplacian of the electron density and the kinetic energy at the bond critical point located for each interaction.

Interaction	ρ	$\nabla^2\rho$	G
BCP in the dimer			
Hg1-Hg2	0.086	0.155	0.064
Hg1-O1 (Hg-$O_{COOshort}$)	0.088	0.437	0.120
Hg1-O2 (Hg-$O_{COOlong}$)	0.027	0.090	0.023
BCP tetramer formation			
Hg1-O6 (Hg-$O_{COO(in)}$)	0.021	0.074	0.018
BCP chain formation			
Hg1-O5 (Hg-$O_{COO(out)}$)	0.015	0.042	0.011
Hg···π	0.009	0.025	0.005
BCP with dioxole(1)			
Hg2-O4 (Hg-O_{diox1})	0.011	0.033	0.008
BCP with dioxole(2)			
Hg1-O7 (Hg-O_{diox2})	0.013	0.037	0.009

References

1 G. M. Sheldrick, *Acta Crystallogr. Sect. A Found. Crystallogr.*, 2008, **64**, 112–122.

2 C. F. MacRae, I. Sovago, S. J. Cottrell, P. T. A. Galek, P. McCabe, E. Pidcock, M. Platings, G. P. Shields, J. S. Stevens, M. Towler and P. A. Wood, *J. Appl. Crystallogr.*, 2020, **53**, 226–235.

3 P. Ugliengo, D. Viterbo and G. Chiari, *Zeitschrift für Krist. - Cryst. Mater.*, 1993, **207**, 9–23.

4 Persistence of Vision Pty. Ltd., 2004.

5 P. R. Spackman, M. J. Turner, J. J. McKinnon, S. K. Wolff, D. J. Grimwood, D. Jayatilaka and M. A. Spackman, *J. Appl. Crystallogr.*, 2021, **54**, 1006–1011.

6 A. D. . Becke, *Phys. Rev. A*, 1988, **38**, 3098–3100.

7 C. Lee, W. Yang and R. G. Parr, *Phys. Rev. B*, 1988, **37**, 785–789.

8 S. Grimme, *J. Comput. Chem.*, 2012, **27**, 1787–1799.

9 R. Krishnan, J. S. Binkley, R. Seeger and J. A. Pople, *J. Chem. Phys.*, 1980, **72**, 650–654.

10 R. Weihrich, I. Anusca and M. Zabel, *Allg. Chem.*, 2005, **631**, 1463–1470.

11 A. Giordana, E. Priola, S. Pantaleone, L. Andreo, L. Mortati, P. Benzi, L. Operti and E. Diana, *Dalton Trans.*, 2022, **51**, 5296–5308.

12 F. Sánchez-Férez, X. Solans-Monfort, T. Calvet, M. Font-Bardia and J. Pons, *Inorg. Chem.*, 2022, **61**, 4965–4979.